Single-molecule analysis of kinesin motility reveals regulation by the cargo-binding tail domain

Dara S. Friedman* and Ronald D. Vale†*‡

**Department of Cellular and Molecular Pharmacology, University of California, San Francisco, California 94143, USA*
†The Howard Hughes Medical Institute, University of California, San Francisco, California 94143, USA
‡e-mail: vale@phy.ucsf.edu

Conventional kinesin transports membranes along microtubules *in vivo*, but the majority of cellular kinesin is unattached to cargo. The motility of non-cargo-bound, soluble kinesin may be repressed by an interaction between the amino-terminal motor and carboxy-terminal cargo-binding tail domains, but neither bead nor microtubule-gliding assays have shown such inhibition. Here we use a single-molecule assay that measures the motility of kinesin unattached to a surface. We show that full-length kinesin binds microtubules and moves about ten times less frequently and exhibits discontinuous motion compared with a truncated kinesin lacking a tail. Mutation of either the stalk hinge or neck coiled-coil domain activates motility of full-length kinesin, indicating that these regions are important for tail-mediated repression. Our results suggest that the motility of soluble kinesin in the cell is inhibited and that the motor becomes activated by cargo binding.

Conventional kinesin is a motor protein that transports membrane-bound organelles[1,2] and intermediate filaments[3,4] along microtubules. Native kinesin is composed of two heavy chains (each of relative molecular mass (M_r) ~120,000 (120K)) and two light chains (M_r~60K–70K)[5,6]. Each heavy chain is divided into four domains, namely the motor catalytic core, neck, stalk and tail (Fig. 1a). The motor catalytic core contains the sites for ATP and microtubule binding[7]. The adjacent neck is divided into two regions, a β-sheet linker involved in motor mechanics and in determining the direction of kinesin movement on the microtubule[8–10], and a coiled-coil domain whose function is not well understood. Between the neck and stalk domain is a predicted unstructured region that may act as a hinge (hinge 1). The stalk comprises two coiled-coil domains separated by a second hinge (hinge 2) that is thought to allow kinesin to fold in half[7,11,12]. The kinesin light chains bind to the carboxy-terminal end of the second stalk coiled-coil[13,14]. Finally, the C-terminal region of the kinesin heavy chain and the light chain together form a globular tail domain that may bind to cargo[7,11,15].

A large proportion of cellular kinesin is not cargo bound[14,16,17]. The presence of this soluble pool has led to the proposal that non-cargo-bound kinesin might be enzymatically inactivated[18]. In support of this hypothesis, soluble kinesin is less active in a microtubule-stimulated ATPase assay than kinesin attached to beads[19,20]. Several results indicate that tail–motor interactions may mediate the inhibition of non-cargo-bound kinesin ATPase activity[11,18]. First, electron microscopy reveals that, at physiological ionic strength, kinesin is folded at hinge 2 such that the head and tail are in close proximity[11,12]. Second, removal of the tail promotes kinesin binding to microtubules[21] and increases microtubule-stimulated ATPase activity[21,22]. Third, the microtubule binding[14] and ATPase[23] activities of the motor domain have been shown to be repressed further by the light chains bound to the heavy-chain tail.

The effect of the tail domain on kinesin motility has been difficult to assess. Native kinesin[23–25] or bacterially expressed, tail-less kinesin dimers[26,27] bound to glass surfaces or carboxylated beads produce similar motility; however, adsorption of the tail domain onto surfaces may alter kinesin's conformation and derepress motor activity. To address this problem, we measured processive motility of full-length and truncated kinesin in solution using a single-molecule fluorescence assay[28].

Table 1 ATPase turnover and microtubule-gliding velocities of kinesins

Kinesin construct	Microtubule-gliding speed (μm min^{-1})	ATPase turnover (k_{cat}) (ATP s^{-1} head^{-1})
K560	39.8±3.1	21.9±2.1
K963	46.6±3.3	6.5±0.6
K963/LC	36.9±10.5	4.5±2.4
K963(Δ505–610)	42.1±5.3	15.7±4.6
K963 (neck mut.)	46.0±2.9	16.4±4.8

Microtubule-gliding assays and microtubule-stimulated ATPase assays were carried out as described in Methods. For microtubule gliding, mean velocities±s.d. are shown for >20 microtubule measurements. The ATPase k_{cat} was derived from a hyperbolic curve fit of ATPase rates at varying microtubule concentrations. The mean and standard deviations obtained from study of two protein preparations are shown.

Results

Expression and activity of kinesin homodimers and heterotetramers. To study the effect of the kinesin tail on motor activity, we prepared three amino-terminally His_6-tagged kinesin constructs, namely full-length heavy chain with and without kinesin light chains (K963 and K963/LC, respectively), and a truncated heavy chain that terminates in the hinge-2 region (K560) (Fig. 1). We first determined the ATPase activity and motility of the baculovirus-expressed kinesins (Table 1). The k_{cat} for microtubule-stimulated ATPase activity of K560 was 21.9±2.1 ATPs hydrolysed per second per head (mean±s.d.), which is similar to values obtained for a C-terminally histidine-tagged K560 protein expressed in bacteria[29]. The k_{cat} values for K963 and K963/LC were 3.4- and 4.9-fold lower than that for K560, respectively, but similar to those obtained for the native kinesin molecule purified from bovine brain[23,30]. These results, as well as others[21], indicate that the tail domain represses the ATPase activity of the motor domain.

In contrast to the ATPase results, however, full-length (K963 and K963/LC) and truncated (K560) kinesins transported microtubules at similar rates in a gliding assay in which the motors were adsorbed onto the surface of a glass coverslip (Table 1). Similar numbers of microtubules were moving, and the motion was smooth for all three proteins (data not shown). From these results,

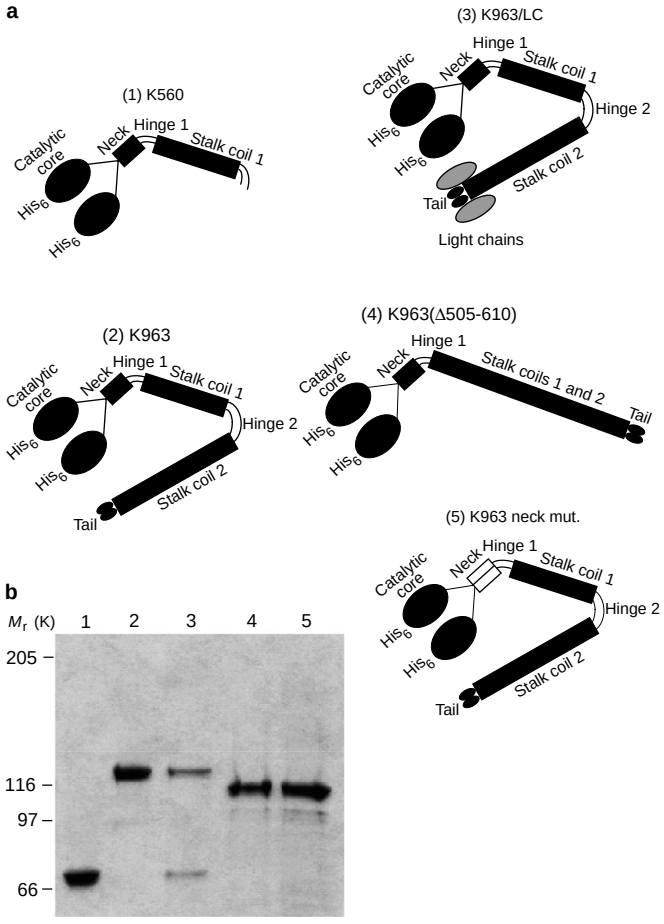

Figure 1 **Domain organization of wild-type and mutant kinesin constructs. a**, Kinesin heavy chains are shown in black and the light chains are grey. All chains have an N-terminal His_6 tag. Protein 1, K560, a homodimer of two kinesin heavy chains truncated at hinge 2. Protein 2, K963, a homodimer of two full-length kinesin heavy chains. Protein 3, K963/LC, a heterotetramer of two full-length kinesin heavy chains and two light chains. Protein 4, K963(Δ505–610), a homodimer of two full-length kinesin heavy chains with hinge 2 deleted. Protein 5, K963 (neck mut.), a homodimer of two full-length kinesin heavy chains with amino acids 337–370 replaced with an artificial, highly stable coiled-coil (indicated by white boxes). The functions of the heavy-chain catalytic core (amino acids 1–322), neck (amino acids 323–371), hinge 1 (amino acids 372–446), stalk 1 (amino acids 447–504), hinge 2 (amino acids 505–605), stalk 2 (amino acids 606–803) and tail (amino acids 804–963) are described in the text and elsewhere[37]. Ovals represent globular domains and rectangles indicate predicted α-helical coiled-coils. **b**, Purified baculovirus-expressed kinesin proteins analysed by SDS–PAGE. Lanes 1–5 correspond to the numbering of the constructs above. Proteins were prepared as described in Methods. Velocity sedimentation analysis confirmed that K560 and K963 are homodimers and that K963/LC is a heterotetramer[18] (data not shown). A 1:0.93 stoichiometric ratio of the heavy and light chains was determined by Coomassie-staining intensity of the two bands on polyacrylamide gels. K963 (neck mut.) has the same predicted molecular weight as wild-type K963, but it migrates more quickly.

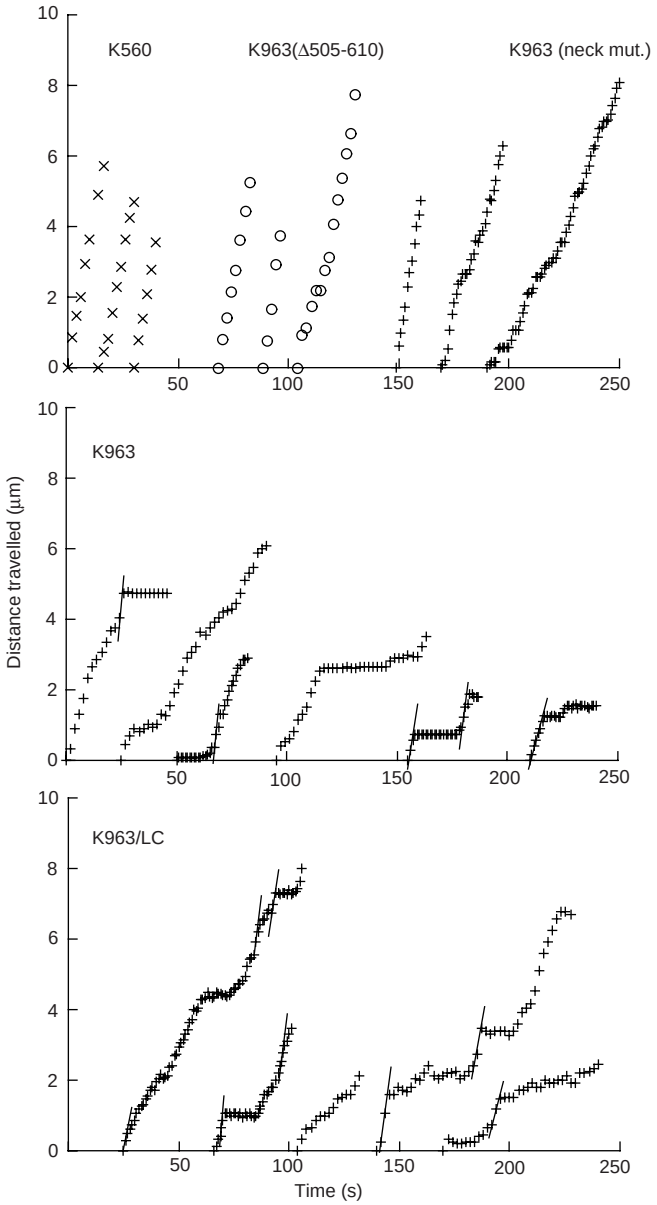

Figure 2 **Tracking the movement of single kinesin molecules.** Representative runs are shown for each construct. Distance travelled was measured every 0.5–2 s until the molecule dissociated from the axoneme or photobleached. K560 and K963(Δ505–610) exhibited smooth motion, whereas K963 and K963/LC exhibited frequent pauses. K963 (neck mut.) runs illustrate both smooth and discontinuous movement, although most of the runs were smooth. Episodes of rapid motion for K963 and K963/LC are highlighted with lines. The highlighted episodes for K963 averaged 14.7 μm min^{-1} and ranged from 7.2 to 20.7 μm min^{-1}; the highlighted episodes for K963/LC averaged 17.1 μm min^{-1} and ranged from 11.0 to 27.9 μm min^{-1}. Episodic velocities were determined with linear regression to three or more consecutive points.

we conclude that our expressed kinesin constructs have active motor domains and behave similarly to native kinesin[25].

Single-molecule analysis of kinesin motility. The finding that full-length kinesin is fully active for motility yet exhibits a low ATPase rate could result from differences in the conformation of the protein between the two assays. Whereas kinesin in the solution ATPase assay may assume a folded, inhibitory conformation, the adsorption of kinesin onto glass in the gliding assay may abrogate tail–head binding and thereby activate motility. For this reason, we studied kinesin motility in solution using a total internal reflection microscope. In this assay, axonemes are adsorbed onto a slide, and single fluorescently labelled kinesin molecules from the solution bind to and move along these microtubule substrates.

In the single-molecule solution assay, all three kinesin proteins moved, although there were substantial differences in the number of microtubule associations and processive runs observed. The frequencies of single-molecule motility events of K963 and K963/LC

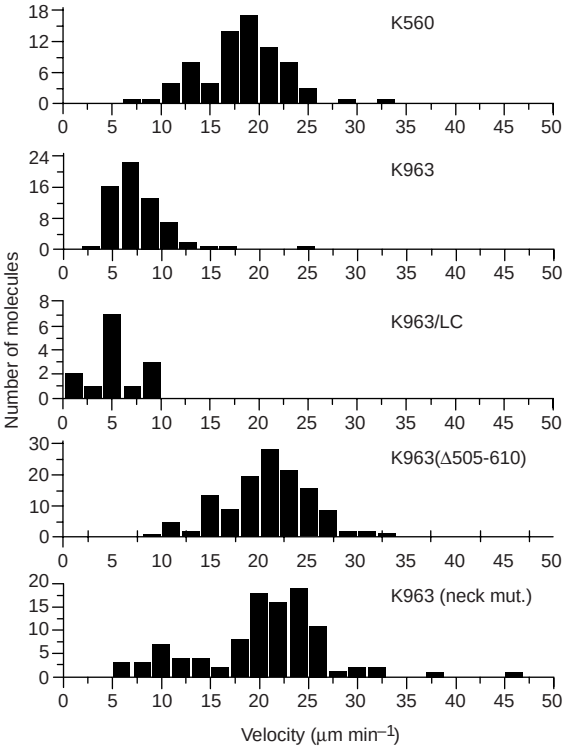

Figure 3 **Histograms of velocities for single fluorescent kinesin molecules.** Velocities of individual Cy3-labelled kinesin molecules moving on axonemes were measured as described in Methods. Episodes in which the motor was paused (stationary) on the axonemes were not included in the analysis.

Table 2 Single-molecule motility measurements

Kinesin construct	Velocity (μm min^{-1})	Run length (μm)	Association time (min)	Frequency Prep. 1 (% K560)	Prep. 2 (% K560)
K560	18.3±4.4	1.03±0.01	0.058±0.001	100	100
K963	8.1±3.9	2.55±0.03	0.347±0.006	10.1	2.0
K963/LC	5.5±2.4	1.03±0.04	0.210±0.007	6.9	1.3
K963(Δ505–610)	20.8±4.5	1.39±0.02	0.067±0.001	49.0	114.6
K963 (neck mut.)	20.4±6.6	1.23±0.01	0.056±0.001	19.7	37.7

Single-molecule motility of Cy3-tagged kinesin on sea urchin axonemes in a total internal reflection microscope. For velocity, means±s.d. were derived from the data shown in Fig. 3. Run lengths and association times (combined data of two independent protein preparations) were determined as described in Methods. The errors of the curve fits are shown. Frequencies of binding/movement are shown for two independently prepared protein preparations and are expressed as the percentage of K560 movement, which was analysed in parallel with the mutants. The absolute K560 frequency values for trials 1 and 2 were 0.53 and 0.15 movements per μm axoneme per nM Cy3–kinesin per min, respectively.

were 90–99% lower than that observed for K560 (Table 2). Once bound to the microtubule, all motors moved but exhibited distinct movement characteristics. Single K560 molecules moved smoothly and continuously[28]; in contrast, the full-length kinesins exhibited discontinuous movement consisting of pauses and bursts of unidirectional motion (Fig. 2). Between pauses, the velocities of motion also differed: heterotetrameric (K963/LC) and homodimeric (K963) kinesin moved 3.3- and 2.3-fold more slowly, respectively, than K560 (Table 2, Fig. 3). To determine whether the slower overall velocity of the full-length kinesins was due to discontinuous motion or reflected differences in intrinsic motor activity, we tracked displacement within a motility event. In doing so, we found that full-length kinesin molecules moved at velocities similar to that of K560 for short time intervals (Fig. 2). The wide range of instantaneous velocities indicates that single K963 and K963/LC molecules may undergo transitions between active and less active states, most likely due to reversible inhibition by the tail domain.

Although K963 and K963/LC bound and initiated runs infrequently, once engaged these full-length kinesin molecules could maintain attachment to, and undergo processive movement along, the microtubule. The average single-molecule run length of K963/LC was the same as that of K560 (1.03μm), and the K963 run length was even longer (2.55 mm). As a result of their normal or long run lengths and slow velocities, K963 and K963/LC were bound to the microtubule for about six- and threefold longer time intervals, respectively, than K560 (Table 2). The longer run lengths and association times of K963 compared with K963/LC may be due to a microtubule-binding activity attributed to the naked heavy-chain tail[31,32] which could maintain kinesin association with the axoneme during times in which the motor domains are detached.

Mutations in the stalk hinge and neck coiled-coil activate motility. To understand how the tail represses kinesin motility, we prepared mutations that might interfere with this regulatory mechanism and thereby activate motility of full-length kinesin. To test the idea that tail–head interactions are required for repression[11,23], we deleted amino acids 505–610 of the heavy chain to join coil 1 and coil 2 in phase and create a continuous coiled-coil that would eliminate hinge 2 (Fig. 1). We tested this mutant as a full-length homodimer (K963(Δ505–610)), as the light chains are not required for repression of single-molecule motility. The ATPase activity of K963(Δ505–610) was increased 2.4-fold compared with that of wild-type K963 (Table 1). In the single-molecule motility assay, K963(Δ505–610) exhibited similar frequencies, run lengths and velocities of movement to the tail-less K560 (Table 2). In addition, single K963(Δ505–610) molecules moved smoothly, in contrast to the discontinuous motion of wild-type K963 (Fig. 2). These results indicate that deletion of hinge 2 is sufficient to disrupt tail-mediated repression of kinesin motor activity.

It has been suggested that the tail may inhibit motor activity by binding to the neck coiled-coil[22]. To test this idea, we replaced the entire sequence of the native neck coiled-coil (residues 337–370)[33] with five copies of a heptad repeat (AEIEALK) that forms a highly stable coiled-coil[34] (K963 (neck mut.)). A K560 protein that had four of the five heptads of the native neck coiled-coil (amino acids 343–370) replaced with this same stable heptad repeat showed nearly wild-type run lengths and velocities in the single-molecule assay[35]. The properties of K963 (neck mut.) (ATPase activity, single-molecule velocities, run lengths, association times and smoothness of motion) were all more akin to those of the tail-less K560 than to the parent K963 protein (Table 2). However, K963 (neck mut.) did not appear to be as fully derepressed as the hingeless K963(Δ505–610), as the frequency of movement of K963 (neck mut.) was somewhat lower than that of K963(Δ505–610). A subset of K963 (neck mut.) molecules also appeared to be transiently repressed, as indicated by their occasional pausing (Fig. 2) and the bimodal distribution of single-molecule velocities (major and minor peaks centred around 22 and 10μm min^{-1} respectively; Fig. 3). Thus, tail-mediated repression of movement was greatly reduced, but not completely eliminated, by the neck coiled-coil mutation.

Discussion

We have shown here that the full-length kinesins are repressed for motility and that the kinesin light chains contribute to, but are not essential for, this regulation. To explain the fewer processive runs observed for full-length versus tail-truncated motor proteins, we propose that the kinesin tail can inhibit or mask the catalytic core's microtubule-binding site. The tail may also inhibit the catalytic mechanism, as full-length kinesin molecules show discontinuous motion once they attach to the microtubule. Such tail-mediated inhibition may be transitory, as full-length kinesins exhibit short

episodes of motion that are of comparable speed to those of tail-less kinesin. On the basis of these and other enzymatic results[21,22], we conclude that the heavy-chain tail represses both the ATPase and the motile activities of kinesin.

The analysis of mutant kinesins has allowed us to identify regions that are important for motor regulation by the tail domain. Hinge 2 has been proposed to enable head–tail contact by providing a flexible joint that allows folding. Consistent with this idea, deletion of hinge 2 produces a motor with nearly identical motility properties to those of a truncated molecule lacking the tail domain. Given this behaviour, we anticipated that K963(Δ505–610) would exhibit an extended conformation at low ionic strength, in contrast to the folded conformation observed for the wild-type heavy chain[18]. However, velocity sedimentation analysis showed that K963 and K963(Δ505–610) migrated at similar S values under various salt conditions (see Methods). This result indicates that K963(Δ505–610) may assume a compact conformation at low ionic strength, as has been seen for a similar hinge 2 deletion in *Syncephalastrum racemosum* kinesin[36]. Folding at hinge 1 may contribute to this compact conformation[36]. Although determining the precise conformation of K963(Δ505–610) will require further studies, our results imply that the head and tail in K963(Δ505–610) are unable to contact one another in the same manner as in wild-type K963. Thus, hinge 2 appears to have an important role in the regulation of motility by the tail.

We have also tested a proposal that tail-mediated repression occurs through an interaction between the tail and the neck coiled-coil[22]. Consistent with this idea, substitution of the native neck coiled-coil with an artificial coiled-coil sequence caused the full-length molecule to behave more like a tail-less molecule and exhibit smooth and continuous motion. Interestingly, the neck coiled-coil mutation can also activate some motile properties of a tail-less kinesin molecule. The artificial neck coiled-coil in K560 fused to green fluorescent protein (GFP) exhibited a 2.5- and 1.7-fold activation of ATPase activity and frequency of motility, respectively (data not shown), in agreement with results of a similar construct studied in ref. 35. Although the exact mechanism of activation is not clear, these results indicate that the native neck coiled-coil can repress motility by tail-independent as well as tail-dependent means.

The sequence of the neck coiled-coil is highly conserved among conventional kinesins[37]. However, we find that substitution of this sequence with an artificial coiled-coil with radically different sequence and stability properties[34] does not alter maximal motility velocity, processivity or force generation (K. Thorn and R.D.V., unpublished observations). Therefore, the neck coiled-coil sequence does not appear to be essential for motor performance, although the coiled-coil structure is important for obtaining maximal velocity and processivity[35,36]. Instead, our results indicate that the neck coiled-coil sequence has been selected for and conserved for purposes of motor regulation. The neck coiled-coil contains conserved charged residues positioned asymmetrically on its surface[33], which may create a docking site for the tail. The neck also contains conserved residues that destabilize the coiled-coil[34], indicating that partial melting of this structure may be required for tail-mediated repression of motor activity.

On the basis of our single-molecule observations, we would expect that non-cargo-bound kinesin *in vivo* is inhibited from binding to and travelling on microtubules and consuming ATP non-productively. The idea that kinesin–microtubule interactions are repressed in the cell is supported by immunofluorescence studies showing that cellular kinesin is not bound to any significant extent to the microtubule cytoskeleton[31,38]. How, then, is kinesin activated in the cell? Membrane binding occurs through the tail domain of kinesin[15,39], which may prevent the tail from interacting with the motor. Our results further indicate that the catalytic core, neck coiled-coil, stalk hinge and tail are all potential sites for modifying kinesin activity. Kinesin phosphorylation[40,41] or binding of kinesin-associated proteins[42,43] at these sites may activate motility either by changing motor conformation or by facilitating membrane association[40,44]. □

Methods

Expression constructs.

pFastBacHTb (Gibco) was used as a vector for baculovirus expression. This vector adds a linker (MSYY), a His_6 tag, a second linker (DYDIPTT), and a tobacco-etch-virus protease-cleavage site (ENLYPQGAMGS) before the first codon of the kinesin gene. The histidine tag was chosen, in part, because this positively charged tag is unlikely to bind to the basic C-terminal tail domain. Human ubiquitous kinesin heavy chain (K963)[31] was subcloned using a polymerase chain reaction (PCR)-introduced 5′ *Bam*HI site and an endogenous 3′ *Xba*I site. To delete hinge 2, we first identified amino acids 505–605 of the heavy chain as likely to disrupt the stalk coiled-coil by using the coiled-coil prediction program Paircoil (http://nightingale.lcs.mit.edu). To join coil 1 and coil 2 of the stalk and maintain the heptad phase, we deleted amino acids 505–610 by restriction digest using endogenous (nucleotide 1,820) and Quik-Change (Stratagene)-introduced (nucleotide 2,138) *Bcl*I sites. The neck coil mutation was first made in a bacterial K560-GFP construct in which heptad repeats 1–5 of the neck coiled-coil (amino acids 337–370 in human kinesin)[33] were replaced with a more stable coiled-coil sequence containing five repeats of the sequence AIEALKA[34]. This mutation was subcloned into wild-type K963 using *Nsi*I sites at nucleotides 455 and 2,978. A truncated kinesin heavy chain construct (K560) was made by introducing a stop codon after nucleotide 1,994 (amino acid 560) and 5′ *Bam*HI and 3′ *Kpn*I restriction sites by PCR. A ubiquitously expressed human kinesin light chain gene (LC)[45], starting at codon 4, was subcloned into pFastBac using 5′ *Bam*HI and 3′ *Sal*I restriction sites engineered by PCR. The coding region of all expression constructs was sequenced.

Protein expression and purification.

Proteins were expressed by recombining the above baculovirus expression constructs individually with baculovirus DNA and infecting Sf9 cells using the Bac-to-Bac expression system (Gibco). 1 l of Sf9 cells was grown in SFM-900 media to a density of ~2×10^6 cells ml^{-1} and inoculated with virus, to a multiplicity of infection of 0.5, containing one of the heavy-chain gene constructs and, in the case of coexpression, the virus containing LC. After 72 h, cells were collected at 450*g* for 10 min, resuspended in 1.5-fold volume of lysis buffer (50 mM Tris, pH 8, 0.5 M NaCl, 10 mM 2-mercaptoethanol, 1 mM phenylmethylsulphonyl fluoride (PMSF), 10 μg ml^{-1} pepstatin, 10 μg ml^{-1} leupeptin, 1 μg ml^{-1} aprotinin and 20 mM imidazole), frozen in liquid nitrogen and stored at –80 °C. To prepare protein, we thawed the extract rapidly at 37 °C to lyse the cells, added fresh PMSF (1 mM), and centrifuged the lysate at 44,000*g* for 40 min. The soluble fraction was bound in batch to 2 ml Ni-NTA agarose (Qiagen) for 60–90 min, and the resin was loaded into a column and then washed with 60 ml of 20 mM Tris, 0.5 M NaCl, 20 mM imidazole, pH 8, followed by 20 ml of 20 mM Tris, 1 M NaCl, pH 8. His_6-tagged protein was eluted with 20 mM Tris, 0.1 M NaCl, 250 mM imidazole, pH 8. The eluate was diluted with MonoQ buffer (25 mM HEPES, pH 7.4, 1 mM $MgCl_2$, 1 mM EGTA and 1 mM dithiothreitol (DTT)) until the conductivity was less than that of MonoQ buffer with 100 mM NaCl, and the protein was then applied to a 1 ml MonoQ column (Pharmacia). When a 0–1 M NaCl gradient was used, kinesin heavy chain, with or without light chain, eluted at ~0.37 M NaCl. For coexpression of kinesin heavy and light chains, the heavy- and light-chain heterotetramer was separated away from contaminating heavy-chain homodimers on a 5–20% sucrose gradient centrifuged at 68,000*g* for 18 h. All protein preparations were stored in sucrose in liquid nitrogen. Protein concentration was determined as described[29].

Bacterial expression and purification of K560–GFP and K560 (neck mut.)–GFP was carried out as described[35], using a microfluidizer to lyse the cells. To select for active protein, kinesin was microtubule bound and released as described below.

ATPase and microtubule-gliding assays.

ATPase activity was measured using a Malachite green assay[46]. Reactions contained 20–100 nM unlabelled kinesin, varying concentrations of microtubules (ranging from 0 to 30 μM), 2 μM Taxol, and 0.5 mM ATP in BRB12 buffer (12 mM K-PIPES, pH 6.8, 1 mM $MgCl_2$ and 1 mM EGTA). Phosphate release was measured 0, 5 and 10 min after the addition of ATP. k_{cat} values were determined using a hyperbolic curve fit of a plot of microtubule concentration versus ATPase rate. Rhodamine-labelled microtubules were used as a substrate for motility by cover-glass-adsorbed kinesin, as described[29]. The mean motility velocity was determined from measurements of 20 or more gliding microtubules.

Hydrodynamic analysis.

S values were determined in different salt conditions (0, 0.15 M, 0.5 M or 1 M NaCl) by velocity sedimentation on a continuous sucrose gradient, as described[18]. ~850 ng kinesin was mixed with standard calibration proteins (BSA, 4.3S; aldolase, 7.4S; and catalase, 11.3S) and loaded onto 7–20% sucrose gradients[18]. After centrifugation at 135,000*g* for 14 h, fractions were analysed by SDS–PAGE followed by transfer to nitrocellulose. The calibration proteins were localized by Ponceau-S staining and kinesin was detected by immunoblotting using an affinity-purified polyclonal antibody raised against a peptide from the motor domain (amino acids 154–173). K963 and K953(Δ505–610) migrated together under various salt conditions (7.1S, 0 M NaCl; 6.7S, 0.15 M NaCl; 5.5S, 0.5 M NaCl; 4.4S, 1 M NaCl).

Solution-based motility assays.

The motility of single Cy3-labelled kinesin molecules was observed along Cy5-labelled sea urchin axonemes using a total internal reflection microscope. Kinesin was labelled by reacting 75 pmol kinesin with 2.5 nmol Cy3, a monofunctional NHS ester that labels free amino groups, for 10 min on ice, and then quenching the reaction with 50 mM glycine, pH 7. Cy3–kinesin was removed from free dye by binding the motor to microtubules with 1 mM AMP-PNP and then centrifuging the motor–microtubule complex through a cushion of 40% sucrose in BRB12 at 230,000*g* for 5 min. Cy3–kinesin was then released by resuspending the microtubules in 50 μl MonoQ buffer containing 0.2 M KCl and 1 mM ATP for 15 min at room temperature; microtubules were removed by centrifugation as described above. Stoichiometry of labelling was determined by measuring the protein concentration, as described above, and by measuring Cy3 concentration on a fluorimeter using Cy3 standards. Molar stoichiometries of

Cy3:protein ranged from 0.1 to 1.1. This labelling procedure did not appear to affect motor activity, as K560 prepared in this way had single-molecule velocities and run lengths that were similar to those of reactive cysteine-Cy3-labelled[28] and GFP-tagged[47] K560. Preparation[48] and labelling[47] of axonemes has been described. Single-molecule motility assays were done as described[28,47] on a custom-built total internal reflection microscope[28,47]. The intensity of the 514-nm argon laser light before entering the prism was 5 mW. At least one field of five or more axonemes was recorded for 4 min for each assay. As motility was rare for K963 and K963/LC, data were collected for up to 25 min to observe more motility events.

Motility was analysed using an NIH-IMAGE-based measuring program developed by J. Hartman. Segments of videotape were digitally captured at 10 frames s^{-1}, and the run lengths and velocities were determined by marking the binding and dissociation events of a single Cy3–kinesin. Run lengths as short as 0.1 µm could be detected. The mean velocities were determined from at least 14 runs that were >0.5 µm. Runs with pauses (no obvious motion) were measured as only one motility event, but pause times were not included in measurements of velocity. To track single-molecule motility, we measured movement of a single fluorescent spot at 0.5–2-s intervals using a program developed by K. Thorn. The run length was determined by nonlinear least-squares fitting of the cumulative probability distribution to $1–\exp^{(-x/t)}$, where the cumulative probability distribution at value x is defined as the fraction of runs with lengths shorter than x (using a fitting program developed by K. Thorn (K560, n=300; K963, n=69; K963/LC, n=20; K963(Δ505–610), n=146; K963 (neck mut.), n=145). Association times represent the time interval between the appearance and disappearance of a moving single fluorescent spot on the microtubule; data points were calculated as run length/velocity for each motility event greater than 0.5 µm. Frequency of movement was determined by counting the number of motility events on an axoneme and normalizing to axoneme length, amount of Cy3–kinesin and the time of observation.

RECEIVED 29 APRIL 1999; REVISED 11 JUNE 1999; ACCEPTED 19 JUNE 1999;
PUBLISHED 11 AUGUST 1999.

1. Vale, R. D. in *Guidebook to Cytoskeletal and Motor Proteins* 2nd edn (eds Kreis, T. E. & Vale, R. D.) 398–402 (Oxford Univ. Press, Oxford, 1999).
2. Hirokawa, N. Kinesin and dynein superfamily proteins and the mechanism of organelle transport. *Science* **279,** 519–526 (1998).
3. Liao, G. & Gundersen, G. Kinesin is a candidate for cross-bridging microtubules and intermediate filaments. *J. Biol. Chem.* **273,** 9797–9803 (1998).
4. Prahlad, V., Yoon, M., Moir, R.D., Vale, R.D. & Goldman, R.D. Rapid movements of vimentin on microtubule tracks: kinesin-dependent assembly of intermediate filament networks. *J. Cell Biol.* **143,** 159–170 (1998).
5. Bloom, G. S., Wagner, M. C., Pfister, K. K. & Brady, S. T. Native structure and physical properties of bovine brain kinesin and identification of the ATP-binding subunit polypeptide. *Biochemistry* **27,** 3409–3416 (1988).
6. Kuznetsov, S. A. *et al.* The quaternary structure of bovine brain kinesin. *EMBO J.* **7,** 353–356 (1988).
7. Yang, J. T., Laymon, R. A. & Goldstein, L. S. A three-domain structure of kinesin heavy chain revealed by DNA sequence and microtubule binding analyses. *Cell* **56,** 879–889 (1989).
8. Henningsen, U. & Schliwa, M. Reversal in the direction of movement of a molecular motor. *Nature* **389,** 93–96 (1997).
9. Endow, S. A. & Waligora, K. W. Determinants of kinesin motor polarity. *Science* **281,** 1200–1202 (1998).
10. Case, R. B., Pierce, D. W., Hom-Booher, N., Hart, C. L. & Vale, R. D. The directional preference of kinesin motors is specified by an element outside of the motor catalytic domain. *Cell* **90,** 959–966 (1997).
11. Hirokawa, N. *et al.* Submolecular domains of bovine brain kinesin identified by electron microscopy and monoclonal antibody decoration. *Cell* **56,** 867–878 (1989).
12. Hisanaga, S. *et al.* The molecular structure of adrenal medulla kinesin. *Cell Motil. Cytoskeleton* **12,** 264–272 (1989).
13. Diefenbach, R. J., Mackay, J. P., Armati, P. J. & Cunningham, A. L. The C-terminal region of the stalk domain of ubiquitous human kinesin heavy chain contains the binding site for kinesin light chain. *Biochemistry* **37,** 16663–16670 (1998).
14. Verhey, K. J. *et al.* Light-chain dependent regulation of kinesin's interaction with microtubules. *J. Cell Biol.* **143,** 1053–1066 (1998).
15. Skoufias, D., Cole, D. G., Wedaman, K. P. & Scholey, J. M. The carboxyl-terminal domain of kinesin heavy chain is important for membrane binding. *J. Biol. Chem.* **269,** 1477–1485 (1994).
16. Hollenbeck, P. J. The distribution, abundance and subcellular localization of kinesin. *J. Biol. Chem.* **108,** 2335–2342 (1989).
17. Niclas, J., Navone, F., Hom-Booher, N. & Vale, R. D. Cloning and localization of a conventional kinesin motor expressed exclusively in neurons. *Neuron* **12,** 1059–1072 (1994).
18. Hackney, D. D., Levitt, J. D. & Suhan, J. Kinesin undergoes a 9 S to 6 S conformational transition. *J. Biol. Chem.* **267,** 8696–8701 (1992).
19. Jiang, M. Y. & Sheetz, M. P. Cargo-activated ATPase activity of kinesin. *Biophys. J.* **68 (suppl.),** 283–285 (1995).
20. Moraga, D. E. & Murphy, D. B. Kinesin is "inactive" unless bound to a solid support. *Mol. Biol. Cell Abstr.* **8,** 258 (1997).
21. Kuznetsov, S. A., Vaisberg, Y. A., Rothwell, S. W., Murphy, D. B. & Gelfand, V. I. Isolation of a 45-kDA fragment from the kinesin heavy chain with enhanced ATPase and microtubule-binding activities. *J. Biol. Chem.* **264,** 589–595 (1989).
22. Stock, M. *et al.* Formation of the compact conformer of kinesin requires a COOH-terminal heavy chain domain and inhibits microtubule-stimulated ATPase activity. *J. Biol. Chem.* **274,** 14617–14623 (1999).
23. Hackney, D. D., Levitt, J. D. & Wagner, D. D. Characterization of $\alpha_2\beta_2$ and α_2 forms of kinesin. *Biochem. Biophys. Res. Commun.* **174,** 810–815 (1991).
24. Vale, R. D., Reese, T. S. & Sheetz, M. P. Identification of a novel force-generating protein, kinesin, involved in microtubule-based motility. *Cell* **42,** 39–50 (1985).
25. Cohn, S. A., Ingold, A. L. & Scholey, J. M. Quantitative analysis of sea urchin egg kinesin-driven microtubule motility. *J. Biol. Chem.* **264,** 4290–4297 (1989).
26. Yang, J. T., Saxton, W. M., Stewart, R. J., Raff, E. C. & Goldstein, L. S. Evidence that the head of kinesin is sufficient for force generation and motility *in vitro*. *Science* **249,** 42–47 (1990).
27. Berliner, E., Young, E. C., Anderson, K., Mahtani, H. & Gelles, J. Failure of a single-headed kinesin to track parallel to microtubule protofilaments. *Nature* **373,** 718–721 (1995).
28. Vale, R. D. *et al.* Direct observation of single kinesin molecules moving along microtubules. *Nature* **380,** 451–453 (1996).
29. Woehlke, G. *et al.* Microtubule interaction site of the kinesin motor. *Cell* **90,** 207–216 (1997).
30. Wagner, M. C., Pfister, K. K., Bloom, G. S. & Brady, S. T. Copurification of kinesin polypeptides with microtubule-stimulated Mg-ATPase activity and kinetic analysis of enzymatic properties. *Cell Motil. Cytoskeleton* **12,** 195–215 (1989).
31. Navone, F. *et al.* Cloning and expression of a human kinesin heavy chain gene: interaction of the COOH-terminal domain with cytoplasmic microtubules in transfected CV-1 cells. *J. Cell Biol.* **117,** 1263–1275 (1992).
32. Andrews, S. B., Gallant, P. E., Leapman, R. D., Schnapp, B. J. & Reese, T. S. Single kinesin molecules crossbridge microtubules *in vitro*. *Proc. Natl Acad. Sci. USA* **90,** 6503–6507 (1993).
33. Kozielski, F. *et al.* The crystal structure of dimeric kinesin and implications for microtubule-dependent motility. *Cell* **91,** 985–994 (1997).
34. Tripet, B., Vale, R. D. & Hodges, R. S. Demonstration of coiled-coil interactions within the kinesin neck region using synthetic peptides: implications for motor activity. *J. Biol. Chem.* **272,** 8946–8956 (1997).
35. Romberg, L., Pierce, D. W. & Vale, R. D. Role of the kinesin neck region in processive microtubule-based motility. *J. Cell Biol.* **140,** 1407–1416 (1998).
36. Grummt, M. *et al.* Importance of a flexible hinge near the motor domain in kinesin-driven motility. *EMBO J.* **17,** 5536–5542 (1998).
37. Vale, R. D. & Fletterick, R. J. The design plan of kinesin motors. *Annu. Rev. Cell Dev. Biol.* **13,** 745–777 (1997).
38. Pfister, K. K., Wagner, M. C., Stenoien, D. L., Brady, S. T. & Bloom, G. S. Monoclonal antibodies to kinesin heavy and lights chains stain vesicle-like structures, but not microtubules, in cultured cells. *J. Cell Biol.* **108,** 1453–1463 (1989).
39. Bi, G. Q. *et al.* Kinesin- and myosin-driven steps of vesicle recruitment for Ca^{2+}-regulated exocytosis. *J. Cell Biol.* **138,** 999–1008 (1997).
40. Lee, K. D. & Hollenbeck, P. J. Phosphorylation of kinesin *in vivo* correlates with organelle association and neurite outgrowth. *J. Biol. Chem.* **270,** 5600–5605 (1995).
41. Matthies, H. J., Miller, R. J. & Palfrey, H. C. Calmodulin binding to and cAMP-dependent phosphorylation of kinesin light chains modulate kinesin ATPase activity. *J. Biol. Chem.* **268,** 11176–11187 (1993).
42. McIlvain, J. M., Burkhardt, J. K., Hamm-Alvarez, S., Argon, Y. & Sheetz, M. P. Regulation of kinesin activity by phosphorylation of kinesin-associated proteins. *J. Biol. Chem.* **269,** 19176–19182 (1994).
43. Lindesmith, L., McIlvain, J. M., Argon, Y. & Sheetz, M. P. Phosphotransferases associated with the regulation of kinesin motor activity. *J. Biol. Chem.* **272,** 22929–22933 (1997).
44. Hollenbeck, P. J. Phosphorylation of neuronal kinesin heavy and light chains *in vivo*. *J. Neurochem.* **60,** 2265–2275 (1993).
45. Cabeza-Arvelaiz, Y. *et al.* Cloning and genetic characterization of the human kinesin light chain (KLC) gene. *DNA Cell Biol.* **12,** 881–892 (1993).
46. Kodama, T., Fukui, K. & Kometani, K. The initial phosphate burst in ATP hydrolysis by myosin and subfragment 1 as studied by a modified Malachite Green method for determination of organic phosphate. *J. Biochem.* **99,** 1465–1472 (1986).
47. Pierce, D. W. & Vale, R. D. Assaying processive movement of kinesin by fluorescence microscopy. *Methods Enzymol.* **298,** 154–171 (1998).
48. Gibbons, I. R. & Fronk, E. A latent adenosine triphosphatase form of dynein 1 from sea urchin sperm flagella. *J. Biol. Chem.* **254,** 187–196 (1979).

ACKNOWLEDGEMENTS

We acknowlege the members of the Vale laboratory for their help in many aspects of this work. We thank J. Hartman, S. Hopkins, D. Pierce, A. Rudner and K. Thorn for insightful discussion, experimental help, and assistance with the manuscript; C. Hart and J. Ubersax for preparing the K560 (neck mut.) clone; L. Lachman and Y. Cabeza-Alvelaiz for providing the kinesin light chain clone and technical advice. D.S.F. is supported by UCSF Cell Biology Training Grant number T32 GM08120.

Correspondence and requests for materials should be addressed to R.D.V. The protein sequences for human ubiquitous kinesin heavy chain and light chain have been deposited at the Protein DataBank under accession numbers U06698 and L04733, respectively.